CHAPTER THREE

WIRELESS BI-DIRECTIONAL DATA COMMUNICATION

3.1 INTRODUCTION

Within any implantable application the concept of information is a key element that constrains the whole system, whether in terms of control commands or in terms of biological information (e.g. bio-recordings). The usual and rather simple approach is to use hard-wire to interface the implant with the external world. That has been carried out for many years and for some applications, mostly involving acute experiments, this solution may be adequate. Major drawbacks related to implants using wires coming out of the skin are related to (1) risk of infection, (2) patient discomfort and (3) aesthetics. And all this disadvantages play a big roll when long-term chronic implantation is mandatory. This chapter presents the development of several wireless communication systems between an external unit and two different type of implants: (1) a batteryless RF powered device and (2) a battery powered device. Each one refers to a particular project: Pressure sensor-ITUBR and Chemical sensor-MARID respectively and consequently provides the requirements (in terms of bandwidth, distance, power, etc..) that each system demands.

Advanced features of the RF-powered implant are related to high bi-directional full-duplex data-rates at the same time of being RF powered. Concerning the battery-powered implant the advanced features are in terms of micro-power (1μA on-chip receiver) and integration (the only off-chip element is a single coil). Also a novel modulation technique for ultra-low power applications is also presented. Next subsections present some theoretical background and analysis concerning communication technology is presented.

3.1.1 Carrier

There are many constraints related to the carrier frequency that one may take into account when designing a telemetry system. For instance if the power and data are transmitted through the same channel, the decision about choosing the right frequency will be limited by the RF power limitations, already depicted in Chapter two. We have seen that the higher the frequency the higher the radiation absorbed by the tissue. Power signals above 10-20MHz have large effective attenuation making difficult to transmit power. So a single carrier providing both energy and data clearly has a maximum bandwidth restricted by the frequency that produces the maximum levels of absorption tolerated by the standard regulations.

Concerning bandwidth allocation of any bio-telemetry system, the FCC has authorized unlicensed use of the 6765-6795 kHz, 13.553-13.567 MHz, 26.957-27.283 MHz, 40.660-40.700 MHz, 138.2-138.45 MHz and 433.050-434.790 MHz bands for Industrial, Scientific and Medical (ISM) telemetry purposes [1]. Other bands in the microwave region (900MHz and above) are not considered because of the high power required to operate at those frequencies (high absorption, see chapter two table 2-1).

Although this regulation might lead to the use of these particular bands, it is important to recognize that a magnetic transcutaneous link does have a very small radiation factor. Even though large quantities of energy can be transferred to a secondary load, the radiated energy is very small, because most of the field is only near field. In a far-field scenario, the electromagnetic waveform is assumed to be a plane wave and can travel long distances. This is the case of the majority of wireless communication and RF systems. But when the near field component is the only relevant one, all regulations tend to become vague and unclear because the signal decay so fast that can hardly interfere with anything above a wavelength distance.

3.1.2 Modulation

Modulation theory provides insights on the basic tradeoff of transmitter power efficiency versus bandwidth efficiency. Modulation design is primarily concerned with the tradeoff of signal power versus error rate over a band-limited noisy channel. This provides an insight into saving transmitted signal power, which saves battery power and prolongs the lifetime of the implant.

Following is a brief description of the modulation techniques available for bio-telemetry and a comparison of their theoretical power efficiency.

i) Amplitude Shift Keying (ASK): Is a special case of Amplitude Modulation where the binary values are represented by two different amplitudes of the carrier frequency. It can be described by:

$$f_c(t) = \begin{cases} A\cos(\omega_c t), & b = 1 \\ 0, & b = 0 \end{cases}$$

Taking the Fourier transform, we obtain:

$$F_c(\omega) = \frac{A}{2}\left[F(\omega - \omega_c) + F(\omega + \omega_c)\right]$$

The effect is to shift the spectrum of the base band signal up to frequency ω_C with symmetrical side bands around ω_C. The transmission bandwidth is twice the initial base band bandwidth.

ii) Frequency Shift Keying (FSK): The carrier alternates between two frequencies, where ω_1 corresponds to a binary 1, and ω_2 to a binary 0. It can be described by:

$$f_c(t) = \begin{cases} A\cos(\omega_1 t), b = 1 \\ A\cos(\omega_2 t), b = 0 \end{cases}, \text{ for } -T/2 \le t \le T/2$$

where T is the base band pulse width. The frequency spectrum of FSK is difficult to obtain. A special case using a sequence of alternating 1's and 0's leads to a good rule of thumb for FM bandwidth and is much easier to evaluate [2]. If the two frequencies are synchronized in phase and given by

$$f_1 = m/T, \text{ and } f_2 = n/T,$$

where *m,n* are integer. The spectrum is given by

$$\frac{\sin[(\omega_1 - \omega_n)T/2]}{(\omega_1 - \omega_n)T/2} + (-1)^n \frac{\sin[(\omega_2 - \omega_n)T/2]}{(\omega_2 - \omega_n)T/2}, \text{ where } \omega_n = \pi n/T$$

The spectrum can be visualized as two superimposed periodic ASK signals. The bandwidth (to first zero crossing) is then

$$B_t = 2B(1+ ß)$$

where B is the base band bandwidth. The parameter ß is defined as

$$ß = \frac{(f_1 - f_2)/2}{B} = \frac{\Delta f}{B}$$

where Δf is called the *frequency deviation*. This result is also known as Carson's rule. If Δf>>B, the bandwidth approaches 2Δf, and it is called *wide band* FM. The bandwidth is essentially independent of the base band bandwidth. For Δf<<B, the bandwidth approaches 2B, and is called *narrow band* FM. The bandwidth is essentially the same as for ASK, and is determined by the base band signal. The minimum spacing required for non-coherent detection of FSK is 1/T Hertz.

It is the expansion of transmission bandwidth that increases the noise immunity, thus narrow band FSK does not have a SNR advantage over ASK. FSK's constant envelope has an advantage when transmitting through a nonlinear channel, and although implementing ASK is simple, it has relatively poor error performance and susceptibility to fading and non-linearities [3].

iii) Binary Phase Shift Keying (BPSK)– The phase of a constant amplitude carrier is switched between two values corresponding to binary 1 and binary 0 respectively. The two phases are separated by 180°, and can be described by

$$f_c(t) = m(t)\cos\omega_c t, \text{for } -T/2 \le t \le T/2,$$

where T is the base band pulse width, and *m(t)* has values of +1 for a binary 1, and –1 for a binary 0. BPSK is equivalent to a double-side band suppressed carrier amplitude modulation, where cos ω_ct is the carrier and *m(t)* is the modulating signal. It has the same double-side band characteristic as ASK, where the bandwidth is twice that of the base band signal, centered at the carrier f_c.

Differential BPSK (DBPSK) is a non-coherent form of PSK which avoids the need for a phase-coherent reference at the receiver. The input signal is first differentially encoded and then modulated using BPSK. While DBPSK signaling has the advantage of reduced receiver complexity, its energy efficiency is inferior to that of coherent BPSK by about 1dB.

iv) Quadrature Phase Shift Keying (QPSK)– The phase of the carrier takes on 1 of 4 equally spaced values ($\pi/4$, $3\pi/4$, $5\pi/4$, $7\pi/4$), where each phase corresponds to a unique pair of message bits. QPSK has twice the bandwidth efficiency of BPSK, since 2 bits are transmitted as a single modulation symbol. The QPSK signal for this set of symbols may be defined as

$$f(t) = \sqrt{\frac{2E_s}{T_s}} \cos\left[2\pi f_c t + (i-1)\frac{\pi}{2}\right], \text{ where } 0 \le t \le T_s \text{, and } \quad i = 1, 2, 3, 4.$$

where T_S is the symbol duration and is equal to twice the bit period. The bit error probability of QPSK is identical to BPSK, but twice as much data can be sent in the same bandwidth, i.e., QPSK provides twice the spectral efficiency with exactly the same energy efficiency.

v) Modulation Tradeoffs: Power, Noise and Bandwidth

Modulation design is primarily concerned with maximizing the bandwidth efficiency, and minimizing the power required for transmission while maintaining an acceptable bit error rate (BER). The most important parameter in determining the performance of a digital communication system is the signal to noise ratio (SNR). SNR is defined by

$$(S/N)_{dB} = 10\log\frac{S_{power}}{N_{power}}$$

which is the ratio of signal power to noise power in a given bandwidth.

Shannon showed that the theoretical maximum channel capacity, in bits per second (bps) is given by

$$C = B\log_2(1 + S/N)$$

where B is the channel bandwidth in Hertz [4]. In practice, however, only much lower rates are achievable, as this formula only accounts for thermal noise.

A parameter related to SNR is the ratio of signal energy per bit to noise energy per Hertz, E_b/N_o. This ratio is defined as

$$E_b/N_o = (S/N)/(R/B)$$

where R is the bit rate, and the ratio (R/B) is the bandwidth efficiency. E_b/N_o is important because the bit error rate (BER) is a decreasing function of this ratio. As the bit rate R increases, the transmitted signal power, relative to noise, must increase to maintain the required E_b/N_o.

Figure 3-1 shows the probability of bit error P_e versus E_b/N_o for ASK, FSK, BPSK and QSK modulation schemes, assuming coherent detection. As E_b/N_o increases, the error rate drops. For P_e less than 10^{-5}, BPSK/QPSK show a 3dB advantage in SNR over ASK/FSK.

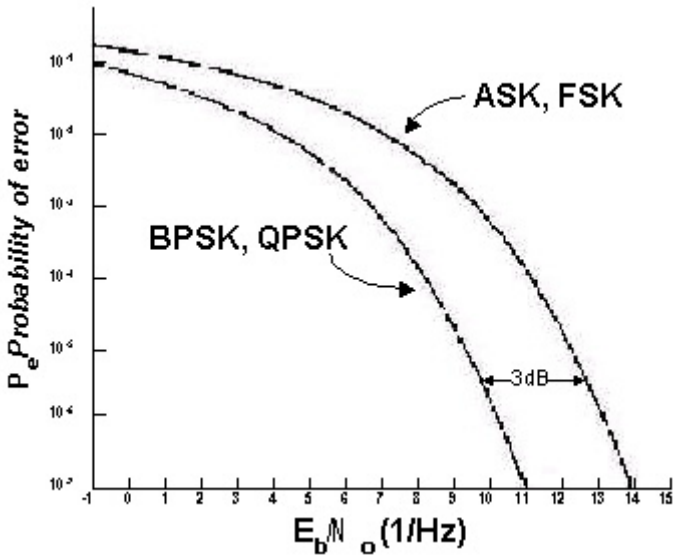

Figure 3-1. Probability of Error vs. E_b/N_o for ASK, FSK, and PSK modulation

Table 3-1 compares ASK, FSK, BPSK and QPSK modulation methods for a 200kbps data rate and BER=10^{-6}. ASK and FSK have the same E_b/N_o performance as well as the same bandwidth efficiency. Both BPSK and QPSK have a 3dB advantage

over ASK/FSK, and QPSK is clearly superior with twice the bandwidth efficiency of BPSK.

Table 3-1. Comparison of various digital modulation schemes

Modulation	Bandwidth (200kbits/sec)	BW Efficiency, R/B (bits/Hz)	E_b/N_o (BER=10^{-6})
ASK	400KHz	0.5	13.5dB
FSK	400KHz	0.5	13.5dB
BPSK	400KHz	0.5	10.5dB
QPSK	200KHz	1.0	10.5dB

3.1.3 Encoding

The transmitted signal power represents just a fraction of the total power required by the communication link. The choice of a modulation scheme should maximize the power efficiency accounting for the power allocation to other subsystems within the link. For example, let's imagine the following case: we have a link where for a QPSK modulator, the output power is around 20% of the total power budget and the modulator itself is around 10%. And now let's imagine we have another option, which is an ASK modulator so simple that have nearly zero cost on the link budget. Even though the transmitter power can be reduced in 3dB in the first case the overall power impact will be only 0.32dB better for the QPSK. Thus, the choice of a modulator is strongly influenced by the implementation complexity and maximum SNR, not as much by theoretical power efficiency of the modulation scheme used.

Base band signals need to be encoded before modulation of the RF carrier. In Pulse Amplitude Modulation (PAM), a series of discrete samples from different analog sources are time-multiplexed into a single stream. Each sample is held for a time **T**, but its value is not quantized nor digitized. Synchronization pulses are usually added to the PAM stream [5]. Passive AM systems has also been reported [6] where a reflected impedance transmitter is used. These systems suffer from fading due to subject movement, usually have poor Signal to Noise Ratio, and only work well with restrained subjects. We will explore this subject more carefully in section 3.2.2.1.

Schemes where the signal voltage is encoded into pulses have also been used extensively. Pulse Width Modulation (PWM) has been used for low data rate transmission of physiological parameters [7], [8]. In PWM each sample of a PAM stream is converted into a pulse with a duty cycle proportional to the sampled voltage. Pulse Position Modulation or Pulse Interval Modulation (PPM/PIM) is a variation of PWM where the information is conveyed in the time between two narrow pulses. In applications with very low data rates this technique achieves significant power savings by turning off the RF oscillator in the interval between the pulses. Power cycling does not work for modulation rates over a few kilohertz because it is very difficult to stabilize a RF oscillator within a fraction of a millisecond. Power cycling also generates spurious signals that can cause serious interference with neighboring transmitters.

Detailed analysis of PWM/PPM signals requires using a double Fourier series expansion in two variables, and is quite complex [9]. A simpler analysis is possible if we consider that a PWM/PPM system must be able to solve the minimum pulse width τ produced by the encoder. The spectrum of a periodic pulse sequence with amplitude A_m, period T, and pulse width τ is given by

$$f(t) = \frac{2}{T}\sum_{n=1}^{\infty}|c_n|\cos(\omega_n t)$$

where $\omega_n = \frac{2\pi n}{T}$,

and $c_n = \tau A_m \frac{\sin\left(\omega_n \tau / 2\right)}{\left(\omega_n \tau / 2\right)}$, for n = 1, 2, 3 ...

The spacing between harmonics is $2\pi/T$. As T decreases the harmonics move farther apart. As the pulse width τ decreases, the first zero crossing moves out in

frequency. For $\tau << T$ most of the signal energy will lie in the range $0 < \omega_n < 2\pi/\tau$. The bandwidth (to the first zero crossing) is thus defined by

$$\omega = \frac{2\pi}{\tau}$$

For example, to transmit 25,000 8-bit samples per second using PWM would require

$$f = \frac{1}{\tau} = \frac{1}{T/2^8} = 25 \times 10^3 \times 256 = 6.4 MHz$$

These pulse techniques, even though adequate for low data rates, are impractical for signals above a few kiloHertz due to the excessive bandwidth required.

In Pulse Code Modulation (PCM), a PAM stream is quantized and digitized by an Analog to Digital converter (ADC). The resulting bit stream is further encoded and shaped to suit the synchronization and RF modulation methods used further downstream. Several PCM biotelemetry systems have been reported in the literature [10][11], [12].

Some advantages of PCM include greater noise immunity and robustness to channel impairments, easier multiplexing of various channels, and ability to accommodate digital error-control codes. PCM also supports complex signal conditioning techniques such as source coding, encryption and equalization to improve the overall performance of the link. This is the encoding technique selected in the telemetry systems implemented into system level.

3.2 CIRCUIT DESIGN AND DEVELOPMENT

This section presents several wireless communication circuits developed in the framework of either RF-powered or battery-powered implants. System level features including communication protocols will be presented in chapter four. The variety of circuits will be presented in terms of its functionality with two major sections:

Downlink communication: defined as data transmitted from the external unit to the implant.

Uplink communication: defined as data transmitted from the implant to the external unit.

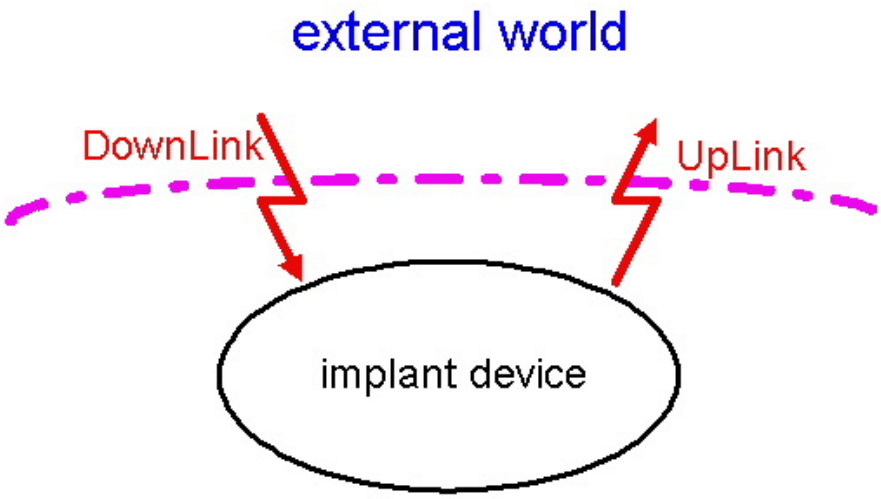

Figure 3-2. Downlink/Uplink in a telemetry system

For the Downlink direction two different schemes were developed. One for a batteryless RF-powered high data rate application and the other one for a battery-powered low bandwidth low-power system. Within each section a description of both external and internal circuits will follow as well as information referred to carrier frequency and modulation technique. For the Uplink direction only one complete data link was developed. Exploration on some additional novel techniques will also be presented.

3.2.1 Downlink communication

Two communication systems were developed. In order to avoid confusion each Downlink system is labeled according to the power technique used. Thus we will talk about a *RF-powered* Downlink and a *battery-powered* Downlink. Both systems had similar constrains in terms of operating distance (10-15mm), although the RF-powered Downlink was designed for high speed data communication and the battery-powered system was designed for ultra-low-power and ultra-integrated features.

3.2.1.1 RF-powered Downlink

The system was developed in the framework of the CNM-ITUBR project, as already mentioned in chapter two. The solution proposed was based in sharing the same carrier signal to send both energy and data. So the Class-E RF transmitter presented in section 2.5 will be modified to include the proper modulation circuit to transmit not only energy but also data.

3.2.1.1.1 Carrier and Modulation

Due to constrains mentioned above the carrier has been chosen taking into account bandwidth limitation, tissue energy absorption and power efficiency fixing the carrier frequency around 10MHz. Another characteristic of the transmitted signal was its big Signal to Noise ratio (for obvious reasons because the carrier was powering the whole implant). Taking into account the transmitter topology, the strong S/N and the simplicity requirement for the implant, the modulation scheme chosen was Amplitude Shift Keying (ASK). Thus modulating the carrier (still keeping a very strong S/N) the receiver was able to demodulate the incoming signal.

3.2.1.1.2 External Transmitter

The Class-E driver was used not only as a RF generator but also as a very efficient AM modulator [13]. The current flowing through the transmitter coil (proportional to the magnetic field generated) follows the Supply Voltage. Thus an amplitude modulation of the Supply induces automatically an amplitude-modulated magnetic field without changing the tuning of the circuit. Next figure shows the ASK modulator in conjunction with the Class-E transmitter (figure 3.3).

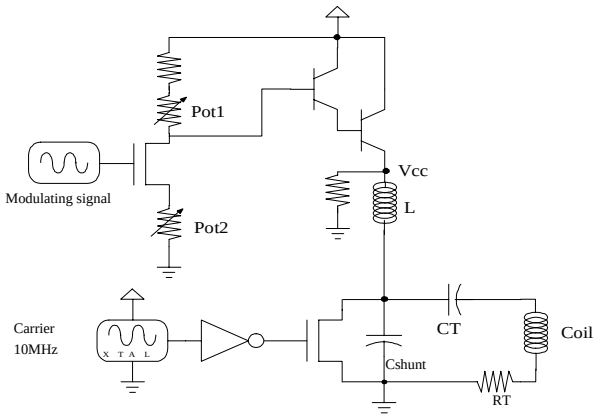

Figure 3-3. ASK modulator within a Class-E transmitter

A variable base voltage in the first bipolar transistor of the Darlington pair defines a variable Vcc voltage that can be adjustable with two potentiometers. Figure 3-4 shows an oscilloscope waveform generated by the ASK transmitter.

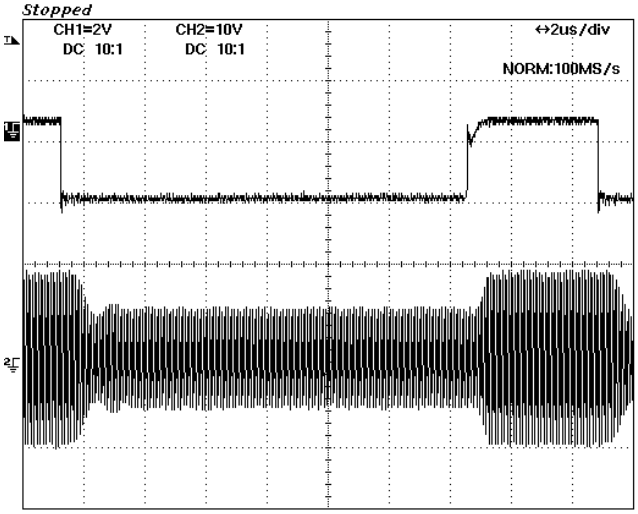

Figure 3-4. ASK modulated coil current

The upper waveform is the modulating signal applied, and the lower waveform is the current flowing through the coil (see figure 3-3). The impact of modulation on the driver efficiency was almost negligible. In order to achieve high data speeds a fast transient was required. A trade-off between bandwidth and efficiency was taken into account, because the Quality Factor (Q) that enhances the efficiency is inversely proportional to the bandwidth (BW). As we can see figure 3-4 (signal with a modulation of 40% and a Q of about 10) the transition between low amplitude to high amplitude was done in about 400ns (scale of time at 2us/div). The transition between high amplitude to low amplitude was done in about 600ns. These values allow theoretical maximum bandwidth near 1MHz.

3.2.1.1.3 Internal Receiver

In order to demodulate the incoming induced voltage an ASK receiver was designed which, in our case, was essentially an envelope detector without AGC (Automatic Gain Control) features. As we can see in next schematic (Figure 3.5.) the induced AC voltage is half-rectified (with an external Schottky diode), high-pass RC filtered (with a peak-detector type of topology including a DC discharge path) and finally Schmitt-triggered with a prior DC-suppresser network.

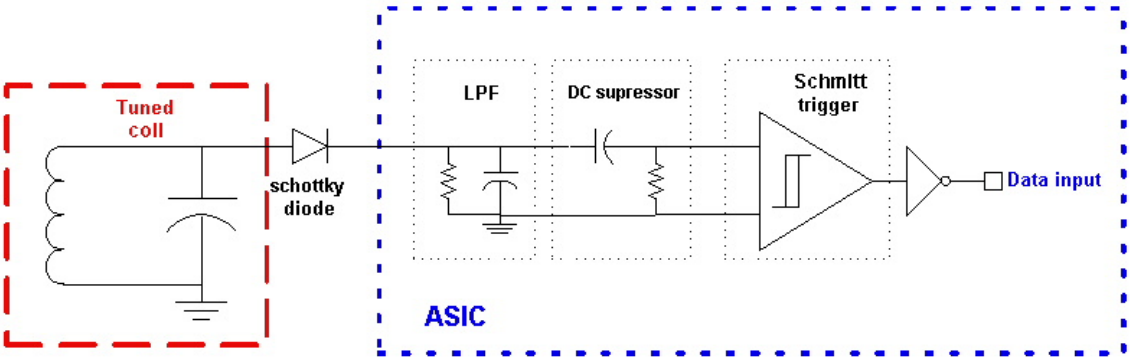

Figure 3-5. ASK receiver

Due to the high signal induced in the coil, no amplifier was required. Thus a simple Schmitt-Trigger was able to provide the digital output of the demodulator. As we see in figure 3-6 and reading from up to bottom and from left to right, the half-rectified 10MHz signal (a) is low-pass filtered rejecting the carrier frequency (b). The third signal

shows a leveled signal without DC (c) and finally the digital Schmitt-Triggered output (d).

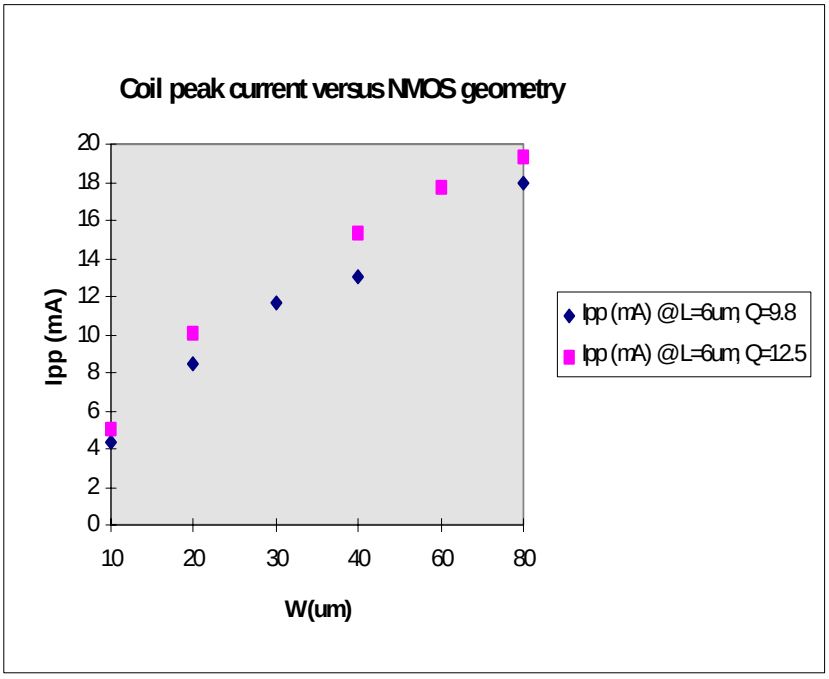

Figure 3-6. ASK signal transmission

The maximum modulation speed one can achieve using this Downlink communication scheme is very much dependent on the coupling factor. For typical conditions of operation (about 10mm distance with 2mm of lateral misalignment maximum) the circuit was able to transmit successfully a digital signal with a frequency above 500kHz (see figure 3-7), which was a "state-of-the-art" value if compared with similar systems [14] [15] by the time this results came out [16]. With a communication channel using clock recovery and no bit codification, possible bit-rates of 1Mbps could theoretically be achieved. This system opened the door to a new generation of high data-rate implants developed in the CNM [17].

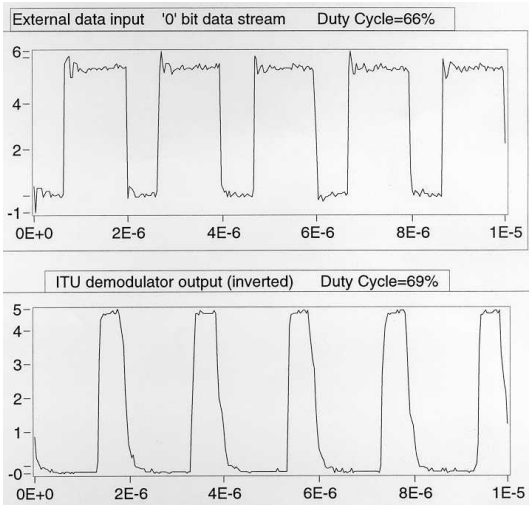

Figure 3-7.30% duty cycle 500kHz Downlink example

When this scheme was applied to the ITUBR system we decided to lower the effective bit-rate down to 250kbps. The reasons were: (1) concerns on coil misalignment and coil-to-coil distance (which can degrade substantially the S/N in the real implant use); (2) the codification scheme used (a return-to-zero pulse-width-modulation that cuts in half the effective bandwidth but simplifies the de-coding and clock recovery circuit) and (3) the fact that the Downlink bit rate requirement for the application was very modest.

Figure 3-8 shows oscilloscope waveforms of a Downlink (ETU→ITU) recorded with the ITUBRv2.0 chip using the ITUBR coding protocol (described in chapter four) for a bit stream at 250kbps..

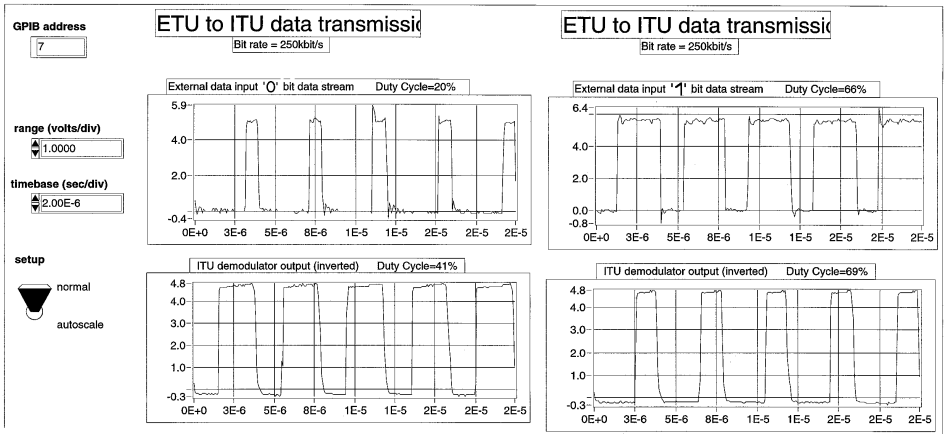

Figure 3-8. ETU to ITU RZ data transmission at 250kbit/s

Every negative edge means a bit change. The upper wave shows the digital signal generated externally which modulates the class-E driver either to generate a ‘0’ (left) or a ‘1’ (right). The lower curve is the output (inverted) of the on-chip ASK demodulator when the chip is already fed by the induced secondary voltage. Besides the time delay between TX and RX signals, we observe a slight variation in the duty-cycle of about 3% for the ‘1’ bit stream (right), but a large change of about 21% in the duty cycle (20% ETU and 41% after ITU demodulation) for a ‘0’ bit stream. That is a very interesting result. The receiver can easily detect a drop in amplitude but takes longer time to detect an increase of amplitude. To solve this problem we could decrease the receiver quality factor, what immediately would help to change faster any received signal, but doing so we would be losing power efficiency. A new technique was used to combine efficiency (high quality facto) and bandwidth. The trick was to over-modulate the transmitted RF signal (20% duty cycle instead of a more relaxed 40%). As we see in figure 3.7 the equivalent 20% ETU duty cycle becomes a 41% ITU duty cycle what makes the communication reliable.

3.2.1.2 Battery-powered Downlink

The Downlink communication system for a battery-powered implant is especially critical. There are two reasons. The first one is power consumption, because we want the implant to be always ready listening to any external command when the device is in total stand-by. And the second one is complexity (which is somehow related to the power and the implant size) especially in case of wide dynamic range of the received signal. In this section a Downlink system for a battery powered implant developed in the framework of the MARID project (see Chapter four) that has overcome the two mentioned problems is presented, featuring a receiver with extremely low power consumption (1μA quiescent) combined with high integration (all-in-ASIC except the coil).

3.2.1.2.1 Carrier and Modulation

A novel idea introduced in this system is the concept of highly de-tuned and virtually loadless receiver. In implants with no external energy needs and with short-distance communication requirements it is possible to use a highly de-tuned and high-impedance receiver in order to have a fully-integrated (except the coil) and frequency independent (up to a certain extend) communication system.

The communication scheme used is On Off Keying (OOK) and is mainly driven by the topology of the receiver (essentially an AC detector).

3.2.1.2.2 External Transmitter

A very similar transmitter topology already presented in the RF-powered system was designed. In this case though, no need of energy was required. As we will see in 3.2.1.2.3. the on-chip receiver was able to detect AC signals if the received amplitude was higher than 200mV and the frequency was higher than 200kHz. The external transmitter built as a demonstrator of the technique was a 1MHz tuned ClassE driver with a very similar coil already used in the RF-powered system. The reason was because in both systems we have very similar distance requirements, and mainly the coil geometry is constrained to distance. For a 1μH coil and a quality factor of 5 we selected the following values for a frequency of 1MHz:

$R=1.1\Omega$ $C_t= 32.6nF$ $C_{shunt}=29.7nF$

With this parameters the transmitter was able to generate a large magnetic field with a modulation index near 100%.

3.2.1.2.3 Internal Receiver

A simple solution to implement an OOK-modulated magnetic field is to use an AC detector, defined as a circuit that triggers a digital value if an AC signal of a certain

magnitude and frequency is applied to the input. Using the ClassE transmitter, for a short distance range and although as we have explained in 3.2.1.2.1. the receiver is out of tune, the S/N and the signal magnitude that the implanted coil receives are large enough to not require any kind of amplification. This is the conceptual approach used in the design of this implanted low quiescent current receiver (Figure 3-9).

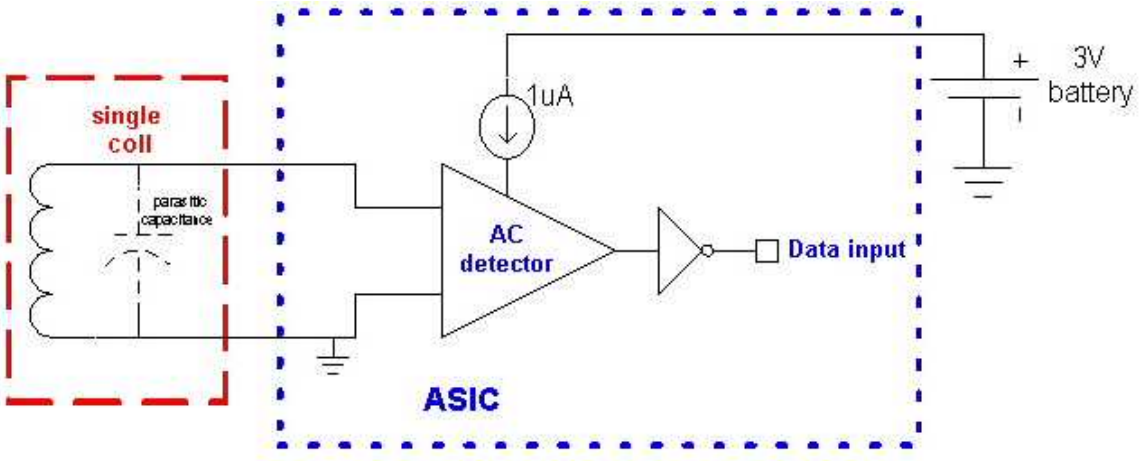

Figure 3-9. Implanted front-end receiver

Next is shown the on-chip receiver with (1) the AC detector and (2) the bias generator:

i) AC Detector design

The Telemetry receiver is essentially an AC detector [18], which combines simplicity and reliability. This is a perfect solution for an OOK modulation scheme especially adequate for short-range communications were the S/N is relatively high. Moreover the detector may be used not only as a communication unit but also as a system wake-up. Next a simplified schematic representation follows:

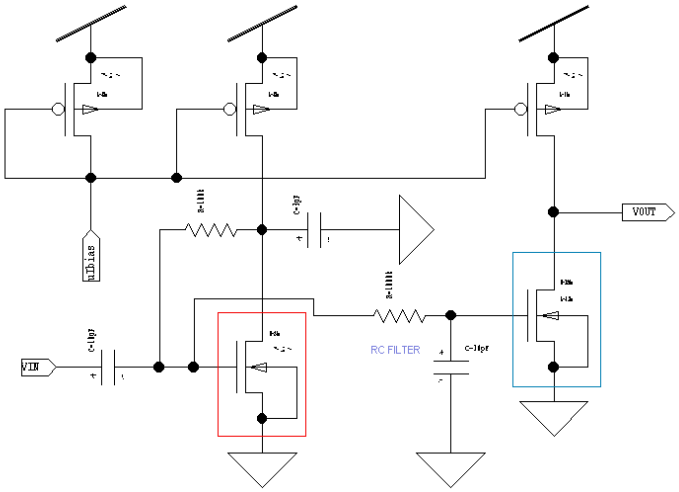

Figure 3-10. AC Detector schematic

Basically the idea is that an increasing input amplitude implies a decrease in the average red-boxed NMOS gate voltage (in order to keep branch current constant) what means a decrease in the gate voltage of the blue-boxed NMOS (after filtering) thus decreasing the NMOS current itself. When this current reach a point were cancels with the PMOS mirror current, then the output capacitance starts to discharge and the output voltage goes to high. Figure 3-11 shows the Post-layout simulation results of the designed AC detector with an inverter buffer output:

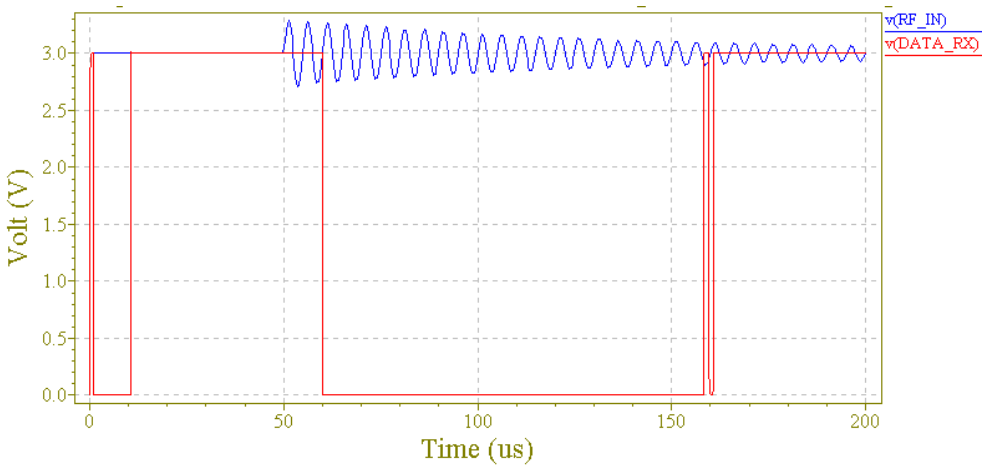

Figure 3-11. AC detector post-layout simulation

Table 3-2 presents some numerical simulation results showing the amplitude and frequency thresholds that apply for different simulation models available:

Table 3-2. Post-layout simulation results

Parameter	BSIM1	BSIM3v3
Amplitude Threshold	130mV	230mV
Frequency Threshold	250kHz	350kHz

So there is dependability in the model. Experimental results show which provides the highest degree of accuracy.

ii) Bias circuit design

In order to achieve ultra-low-power features the biasing circuit is designed specially to give a 200nA current reference. A PTAT reference has been implemented. Its topology allows on-chip resistance values for references ranging from tens of nAs to tens of uAs. Next figure shows a PTAT reference:

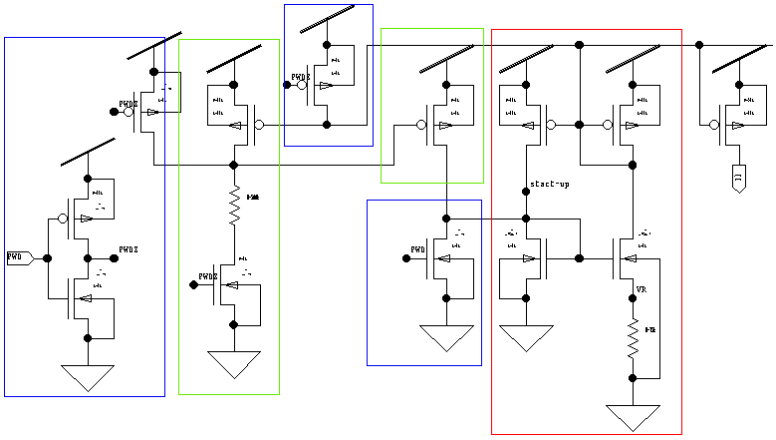

Figure 3.12. PTAT Current reference schematic

In red the PTAT reference (two CMOS branches with a double current mirror). VR (voltage across the resistance) depends mainly on the current-mirror gains. The final IR will be VR/R, which is latter PMOS mirrored to all requested output currents.

There are two steady-states. The first one provides a zero current through the resistance. The second steady-state is the one that provides the nominal bias reference

desired. In order to avoid the first zero-current steady state an automatic self-start circuit is normally added to the reference (in green rectangles), so when a low voltage is sensed in the start-up node the circuit opens a PMOS switch that powers this line to higher values, until it reaches the correct steady state.

In the bias circuit of the receiver the quiescent current limit was so low that even the self-start circuit would be too costly. Moreover as the on/off transition was only possible in the initial power ON of the system (the rest of the time the circuit is continuously fed) a solution to this problem was found adding a single transistor controlled by the power-on reset. This transistor was able to put energy into the start-up node (see figure 3.12) and avoid the zero-current steady state.

iii) Receiver results:

Once the AC detector and the bias circuit were connected together, the overall circuit showed the results presented in table 3-3.

Table 3-3. Receiver experimental results

	Measurements		
Parameter	**chip#1**	**chip#2**	**chip#3**
Quiescent Consumption @ 3V	1µA	1µA	1µA
Amplitude Threshold @ HF	186mV	180mV	180mV
Amplitude Threshold @ 300kHz	210mV	208mV	208mV

With a frequency above the frequency threshold (around 300kHz), the circuit was able to sense any AC signal with a peak amplitude equal or higher than 180mV. For signals getting closer to the frequency threshold, the signal threshold was increasing, with a value around 210mV at a frequency of 300kHz.

In terms of communication with the external transmitter already presented, the system was able to transmit low bandwidth data (up to few kHz) reaching easily a distance of half a meter even for a highly de-tuned 1cm coil.

3.2.2 Uplink communication

Section 3.2.1. was devoted to the Downlink (external to the implant) communication system, showing two different approaches for both, (1) a batteryless RF-powered and (2) a battery-powered implant. Now the communication systems developed to send data from the implant to the external world will be presented. Although major effort was devoted to the development of an active telemetry using BPSK modulation, this section also contains a novel communication technique that uses bursts of energy dumped into a resonant tank (named "LC-modulation") to communicate using PPM with the external world.

3.2.2.1 Active versus passive telemetry

A general concern in all implants is, as we have pointed out in former chapters, the available energy to perform the tasks required. Managing wisely the power also matters when considering the design of a telemetry system. In the Downlink section of this chapter (3.2.1) we have seen two different communication systems (either with or without battery) taking profit of an advantageous signal-to-noise ratio due to (1) the large power available in the external unit and (2) the short distances of transmission. In the Uplink systems we may still have the advantage of short distances but we definitely do not have a large quantity of energy to spend. So the communication strategy will have to be compatible with this constrain.

There are two major ways of achieving a data transmission in the RF-powered scenario (see figure 3-13): (1) the so called *active* telemetry[19][20], where a build-in oscillator generates a radio-frequency signal that is being transmitted to the outside and (2) the *passive* telemetry[21][22], were a load-modulation circuit produces changes in the reflected impedance in a way that can be codified and eventually used as a data transmission system.

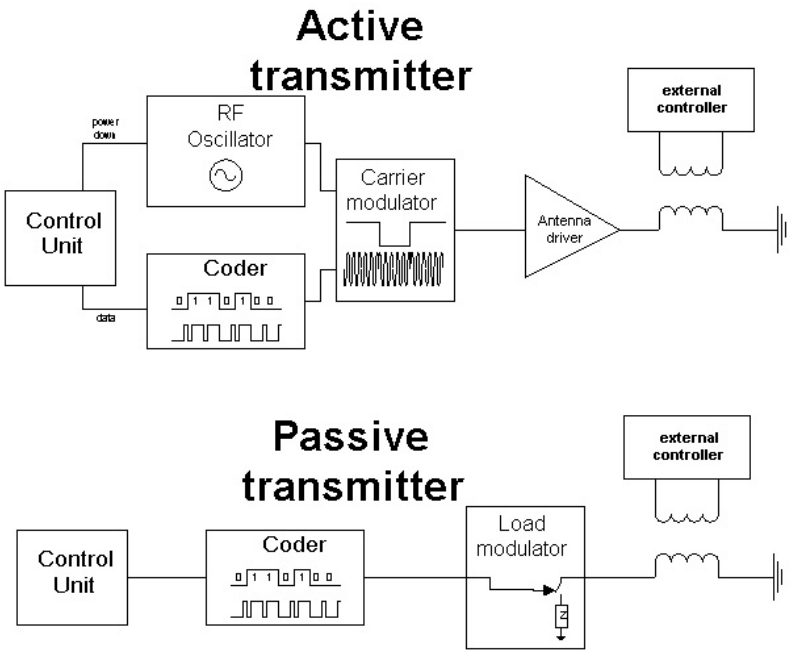

Figure 3-13 Active (above) vs passive (bellow) telemetry schemes

The major advantage of the passive telemetry is simplicity in the transmitter site, although the external receiver can require complex electronics, especially when low coupling factors apply. The active telemetry in the other hand requires an on-chip oscillator and also a coil driver, but can achieve higher degrees of reliability because the system is much less sensitive to distance and misalignment variations. The Uplink circuit presented in this thesis is based in the active telemetry concept.

As mentioned above in a RF-powered system we have the capability of achieve data transmission through an active or passive technique. Both require power. The active telemetry needs obviously to feed a local oscillator and some kind of modulator and amplifier. But also all the passive telemetry technique require power as well, although the name may induce to some misunderstandings. When the passive telemetry modulates the load impedance this normally means: (1) an increase on current demand of the implant (an increase of power consumption increases the reflected impedance in the external coil) or (2) a decrease of energy available due to either detuning or increase of effective secondary load (that actually decreases the reflected impedance). So in either case we are losing power.

The reflected impedance has the following dependence [23]:

$$Z_{ref} = \frac{1}{jwC_p}(1-k^2) + R_{load}k^2\frac{L_p}{L_s}$$

Where C_p is the primary capacitance, L_p is the primary inductance, L_s is the secondary inductance, k is the coupling factor and R_{load} is the secondary load. We observe a quadratic dependence of the reflected impedance with the coupling factor, which at the same time has a very strong decay with distance. That's why the passive technique is only useful if reasonable coupling apply.

In terms of active telemetry there are two major approaches: (1) LF inductive link and (2) HF far-field. Both require an oscillator. The major difference is that the inductive link uses the near-field component (magnetic in most of the cases) as opposed to the HF approach were the wavelength is much smaller than the distance of transmission and the dominant field component is the radiation field. The fast decay of the near field component (as explained in chapter two) makes the HF option especially useful when larger communication distances are required. But high frequencies up to few GHz may well be very expensive (in terms of power and technology) to produce and manipulate. Taking into account that the electromagnetic absorption by the body increases with frequency in most of the cases where short distances apply the low frequency inductive link approach is the most suitable one.

3.2.2.2 Digitally tunable BPSK transmitter

The main Uplink system developed uses the active-inductive link telemetry. This approach was used for all system demonstrators shown in chapter four, both for batteryless or battery powered implants. On the contrary and as we have seen in section 3.2.1 the Downlink uses different schemes for each type of device.

Due to the small amount of energy available in the implant, whichever technique used to communicate will produce a weak signal in the external receiver with a poor S/N. And as we have seen in section 3.1 amplitude modulation is always difficult to implement is such conditions, as opposed to exponential modulation (either phase or frequency) where the information does not relay in the energy (amplitude). The modulation technique used is Binary Phase Shift Keying (BPSK), which provides a low-complexity solution. We will see more details in next sections. The BPSK technique can also be seen as local frequency changes resulting in phase displacement.

3.2.2.2.1 Internal Transmitter

A tiny coil is the magnetic transmitter driven by a pulsed current source with programmable frequency. This capability of changing the frequency allows having a highly tuned transmitter without requiring any off-chip tuning element. Figure 3-14 shows a block diagram of the internal transmitter with the different circuit elements required.

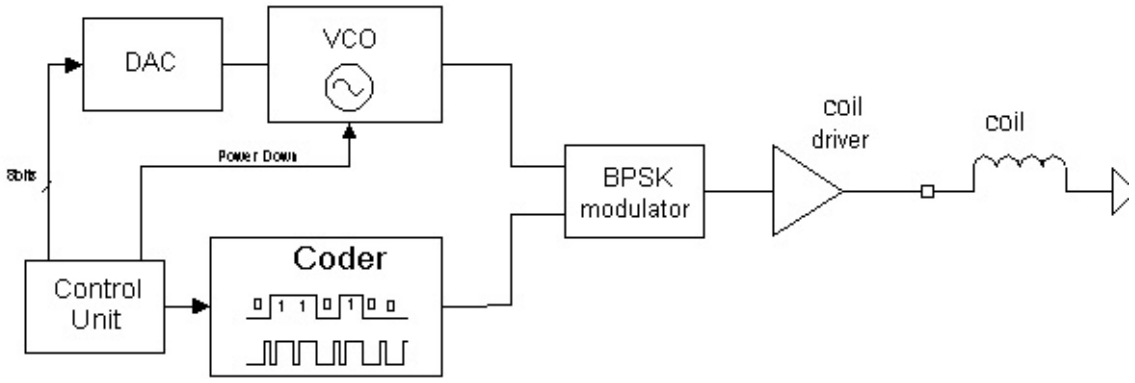

Figure 3-14. On-chip transmitter

A change in the 8-bit DAC input results in a change in the output of the Voltage Controlled Oscillator. So the carrier frequency is adjustable by the control unit. Then the BPSK modulator changes the phase of the carrier 180 degrees every data transition. Finally this modulated signal goes to the coil driver that provides the current to the transmitter coil to generate a large enough magnetic field.

3.2.2.2.1.1 DAC

The 8-bit DAC was implemented using the R-2R topology [24].The linearity depends essentially on the matching between the ladder resistances, and the parasitic resistance due to the switches. In order to obtain good linearity figures a matching analysis was performed. The physical synthesis used poly resistance. Figure 3-15 shows a bit-cell with the matched resistance to the MOS switch.

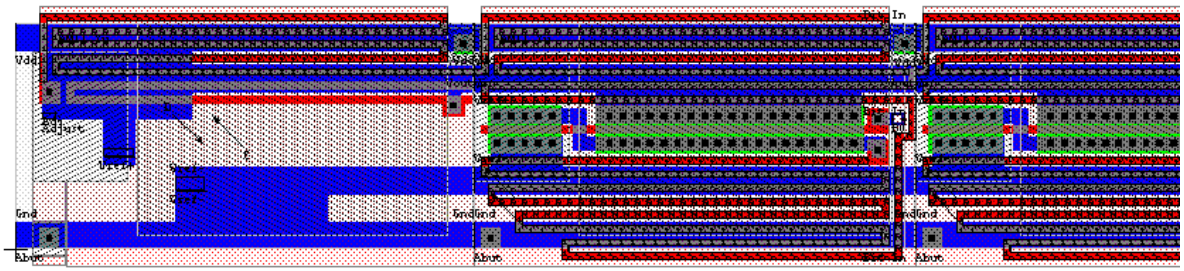

Figure 3-15. R-2R DAC layout optimization

Once fabricated and tested the DAC showed (see figure 3-16) a behavior very close to the simulated result.

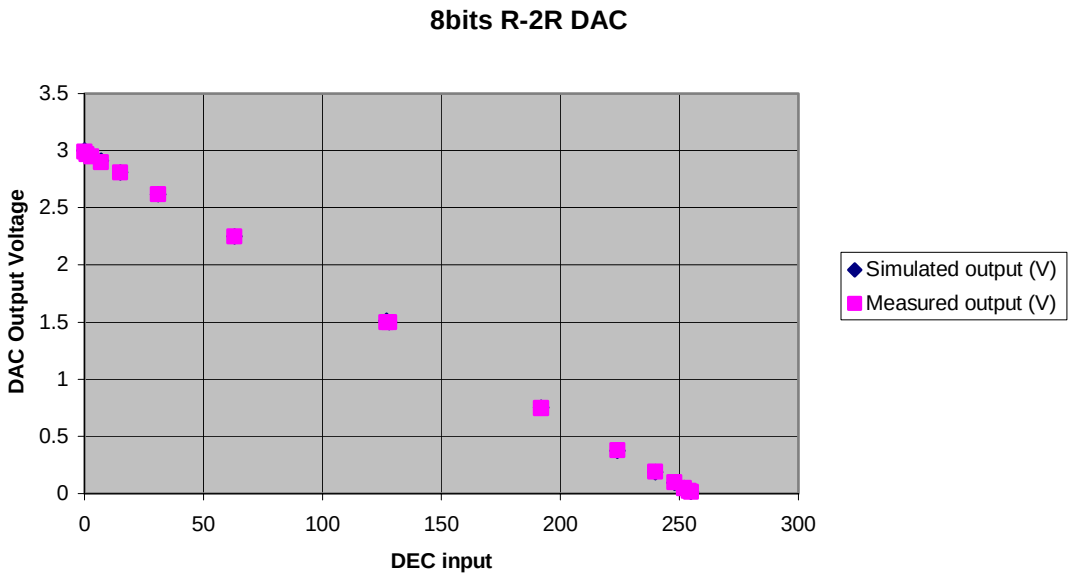

Figure 3-16. DAC experimental results versus simulations

The linearity was successfully achieved in all the supply range.

3.2.2.2.1.2 VCO

The Voltage Controlled Oscillator (VCO) was implemented using the simple principle that in a ring oscillator the frequency depends on the supply voltage. The frequency is indirectly proportional to the time-delay of one inverter, and this time-delay is proportional to the drain-source on-resistance (Rds) which is indirectly proportional to the drain-source voltage (Vdd in the inverter case). Thus the frequency will be proportional to the voltage supply. The draw back of a circuit like this is its intrinsic poor control on the frequency. Although with a proper supply control (DAC output with a buffer) reasonable levels of linearity might be expected.

Figure 3-17 shows a transient post-layout simulation of the VCO. The red curve is the buffered output of the DAC (input of the VCO). The blue trace shows the variable output voltage with a frequency following the input voltage.

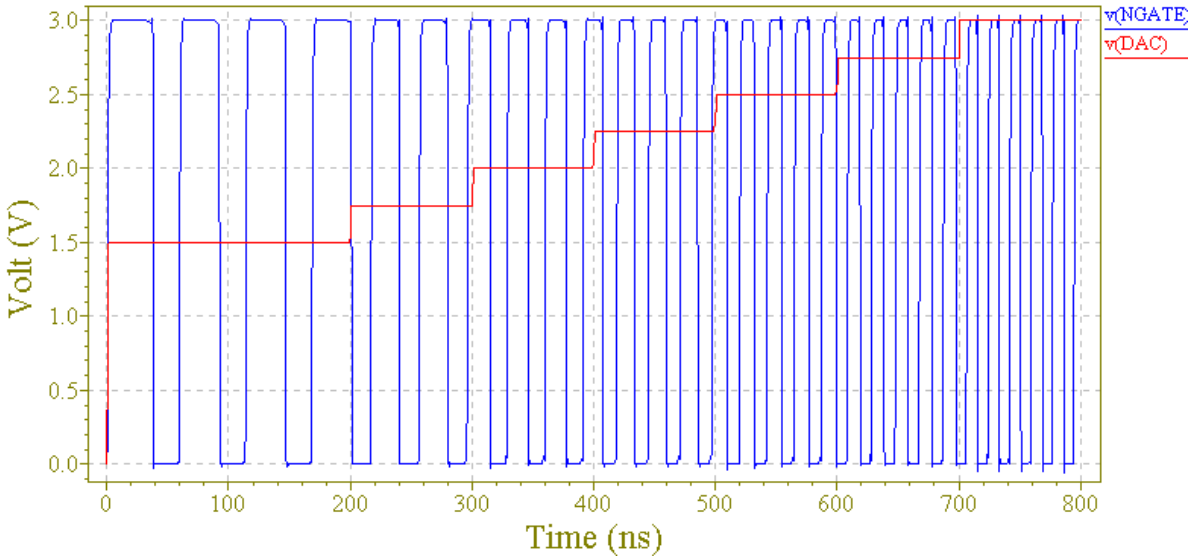

Figure 3-17. Post-layout transient simulation results

Figure 3-18 shows the experimental results of the VCO including the DAC and the buffer: The X-axis is the digital input (in DEC format) and the Y-axis is the output frequency with four different test points.

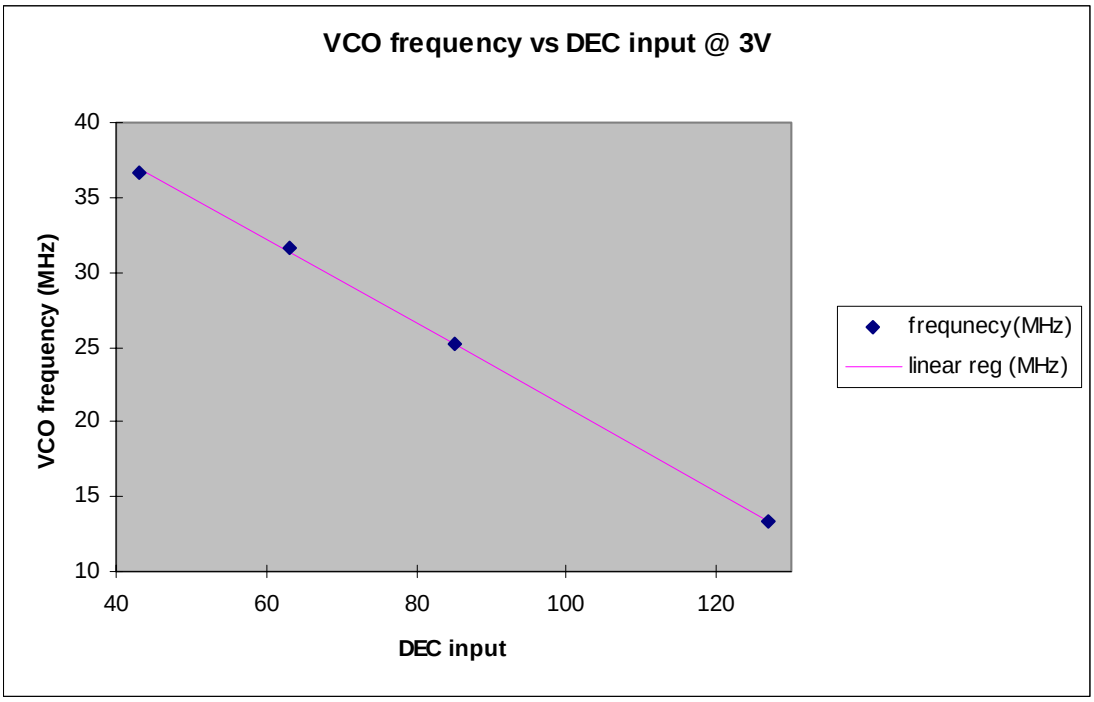

Figure 3-18. VCO experimental results

Linearity again was successfully achieved within the frequency range of interest (15-35MHz).

3.2.2.2.1.3 Modulator and coil driver

Binary Phase Shift Keying was implemented digitally using a XOR gate, mixing the carrier with the data. Every transition in the data line caused a change in 180 degree in the phase of the incoming high frequency digital signal.

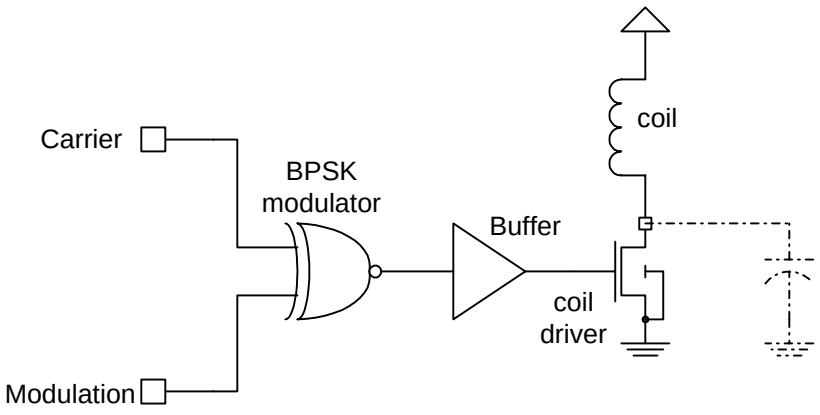

Figure 3-19. Modulator and coil driver

As we see in picture 3-19, the modulated digital signal goes directly to the gate of a NMOS transistor, which acts as a current source driving the resonant coil in a class-B configuration. The almost self-oscillating peak current in the coil depends on (1) the size of the source transistor (which modulates the energy injected in the L tank), (2) the quality factor Q of the coil and (3) the good matching between carrier frequency and coil impedance (figure 3-20).

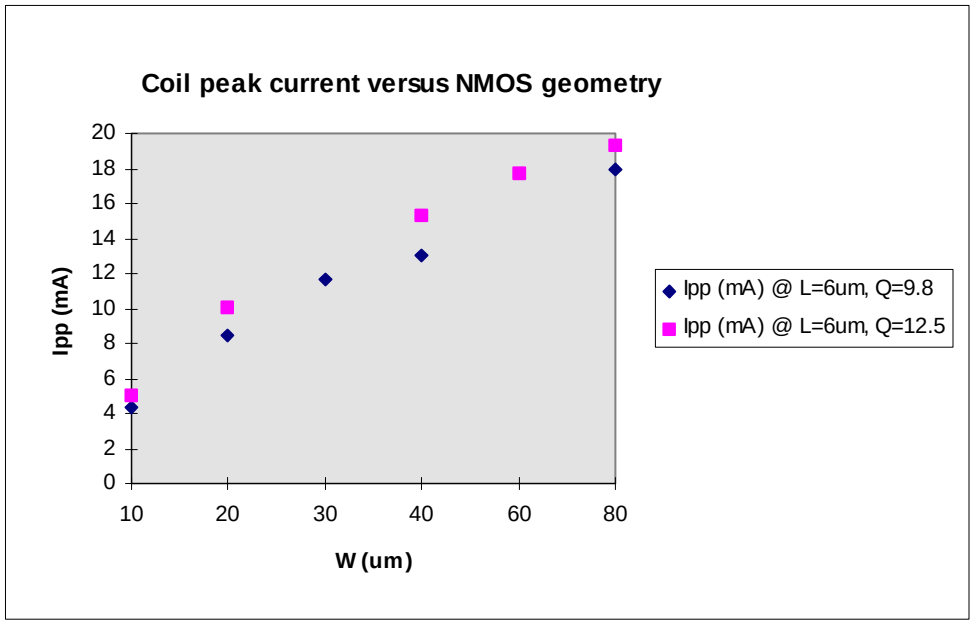

Figure 3-20. Coil peak current vs driver size vs Q

Picture 3-21 shows the modulated coil current for a 28.5MHz carrier, superimposed with a non-modulated 28.5MHz coil current, in order to observe clearly the 180-degree change of phase. We see that the change in phase is also combined with a change in current amplitude, which is very natural, because the phase shift also implies a detuning of the carrier, thus decreasing the impedance matching. In about three cycles, a 180 degrees shift is almost complete, what makes the transmitter suitable for high data rates if required.

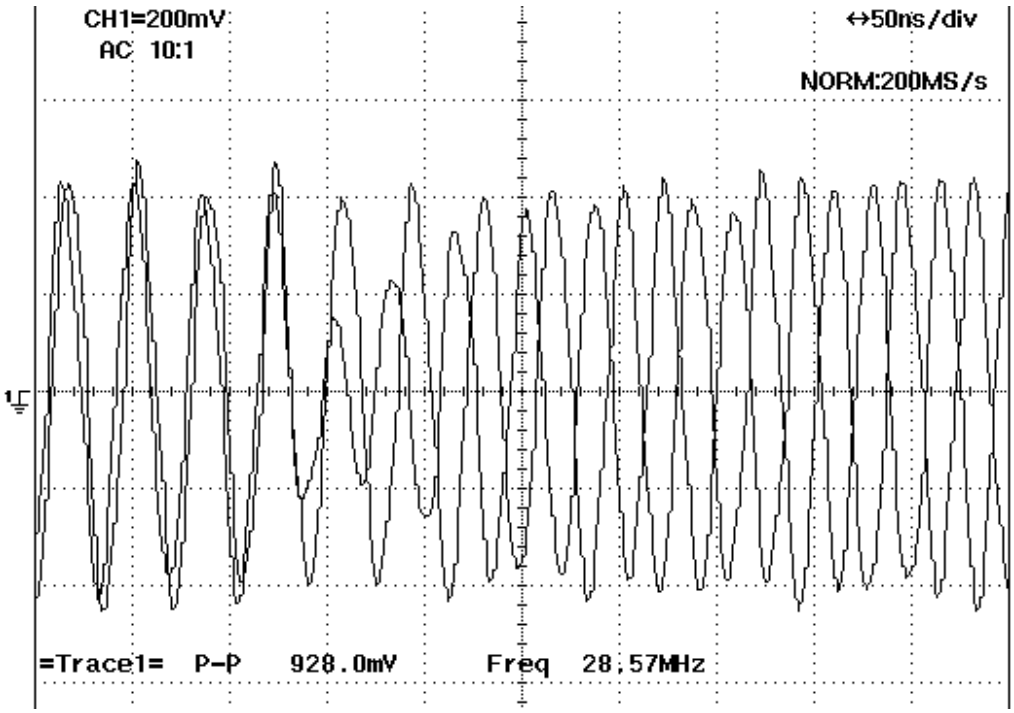

Figure 3-21. Phase shift detail

Table 3-4 shows the coil parameters as well as the frequency, peak current and current supply of the driver:

Table 3-4.On-chip transmitter features

Modulation	Vpp coil	Lt (μH)	Rs (Ω)	Ipp coil	frequency	Current supply
BPSK	950mV	0.42	9	12.6mA	28.5MHz	620uA

3.2.2.2.2 External Receiver

The principle of operation of the receiver is graphically represented in Figure 3-2. A bandpass amplifier first process the incoming signal picked up by the receiver coil. Then the amplifier takes the input signal to a level compatible with the demodulator input. On the other hand it filters out any undesired signal. This filtering feature is especially important in case of RF powering, because a very strong signal coming from the external transmitter will be seen by the external receiver as well.

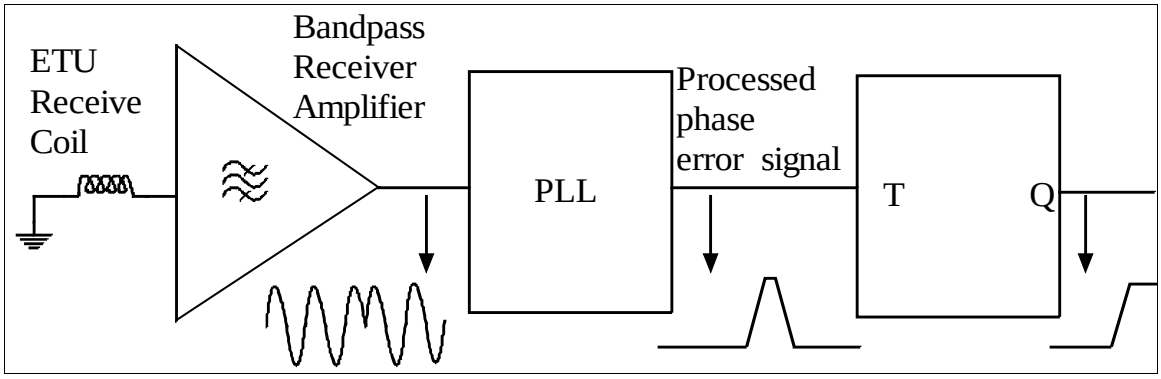

Figure 3-22. Principle of operation

Following the amplifier there is the BPSK demodulator. A simple demodulation scheme, based on the processing of the error signal of a high-speed phase locked loop (PLL) was proposed. The PLL gets back in lock between two-phase transitions and when a transition happens, the resulting phase error signal is processed to obtain a single output pulse per phase transition. These pulses drive a T flip-flop that changes state with each pulse, reconstructing the data. The reconstructed data is either the original data or the inverse of the original data. This ambiguity is inherent to BPSK modulation, where only the transitions in the data are transmitted, but not the original values. Nevertheless the line code chosen to represent the 1 and 0 allows reconstructing the original data, which is done digitally in the external unit (see next chapter, section 4.2.2.2.3.1).

The BPSK demodulator is based on the Phillips NE564 Phase Locked Loop. Its block diagram is shown in Figure 3-23. On of the main features of the circuit is that several PLL parameters can be externally set (such as the free running frequency the loop gain and the loop filter). By doing so we can control the error transient response with a phase input step, so that we get at the output only one pulse per phase change. On the other hand the NE564 includes a filter amplifier and output Schmitt trigger comparator with programmable hysteresis that allow processing the error signal to obtain the desired result.

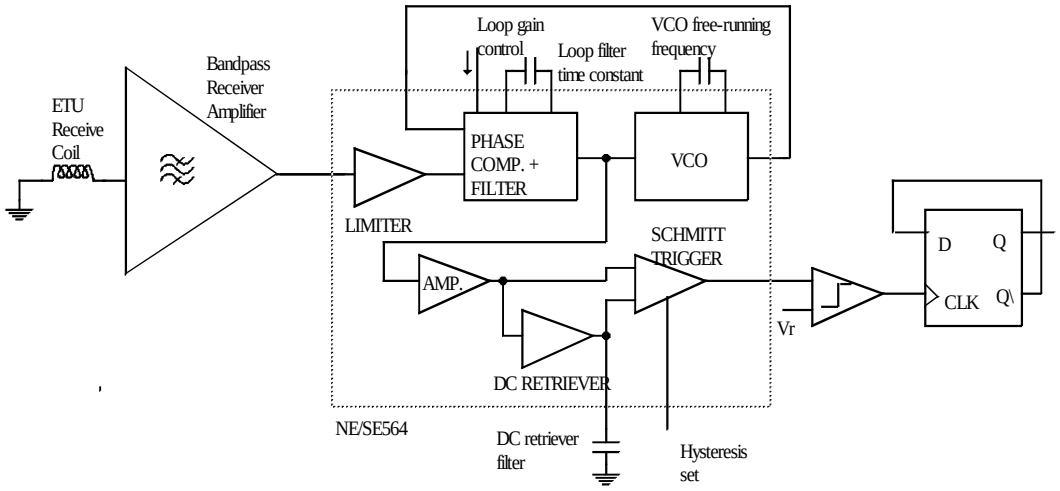

Figure 3-23. BPSK demodulator

At the output of the PLL the signal is further processed with a comparator to obtain clean clock pulses for the T flip-flop.

Figure 3-24 shows the processed phase error signal of the PLL in the receiver versus the input data in the transmitter at a distance of 10mm.

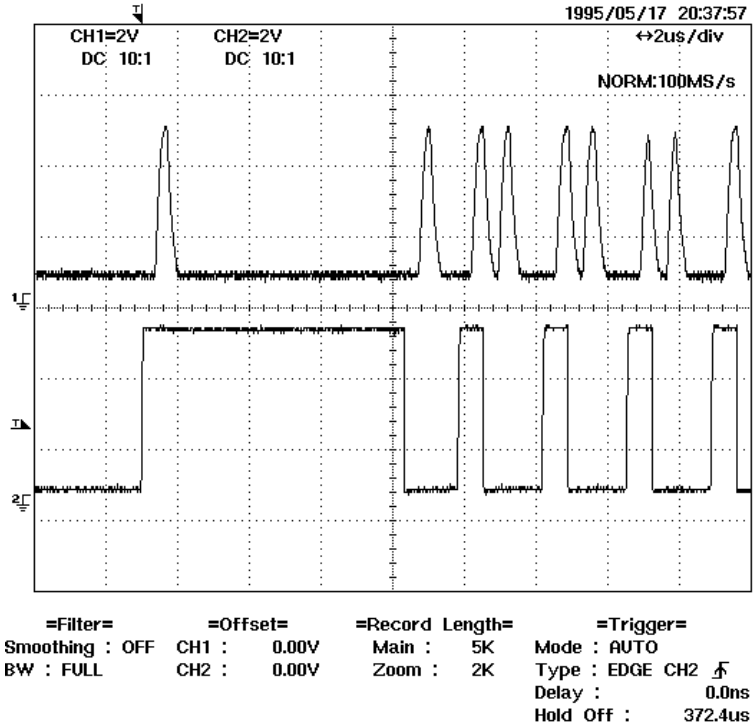

Figure 3-24. BPSK demodulator PLL error signal vs TX data

As we see, every time there is a transition between low to high or high to low in the incoming data a burst is generated in the PLL. Due to the fast phase transition and the high carrier frequency, high data rates can be achieved. In this particular case, using a Return-to-zero (RTZ) bit codification (see section 3.2.1.1.3. and chapter four), the bit rate is 434kbps. Once a clear signal come out of the PLL a trigger circuit construct the exact data signal transmitted to the implant. Figure 3-25 shows a TX data stream and its data received counterpart:

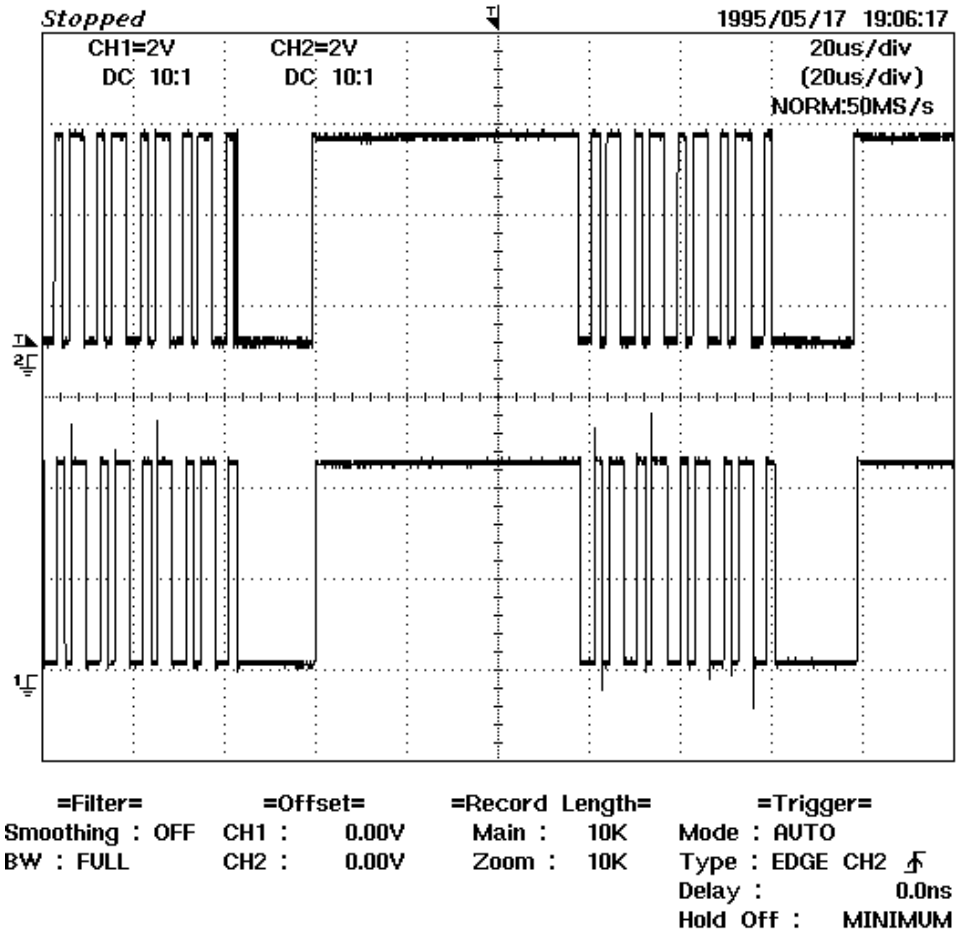

Figure 3-25. Transmitted versus received data stream

The upper signal is the transmitted-internal signal and the lower part is the received and demodulated external data stream, with a coil-to-coil distance of 5cm.

3.2.2.3 Other proposals

3.2.2.3.1 OOK-modulation

The results and techniques presented so far were implemented within a real implantable system, as we will see in next chapter. But in the course of the research, several other techniques were investigated, for example passive telemetry, or other types of active telemetry like On-Off Keying (OOK). Next picture shows a received OOK signal in the external unit.

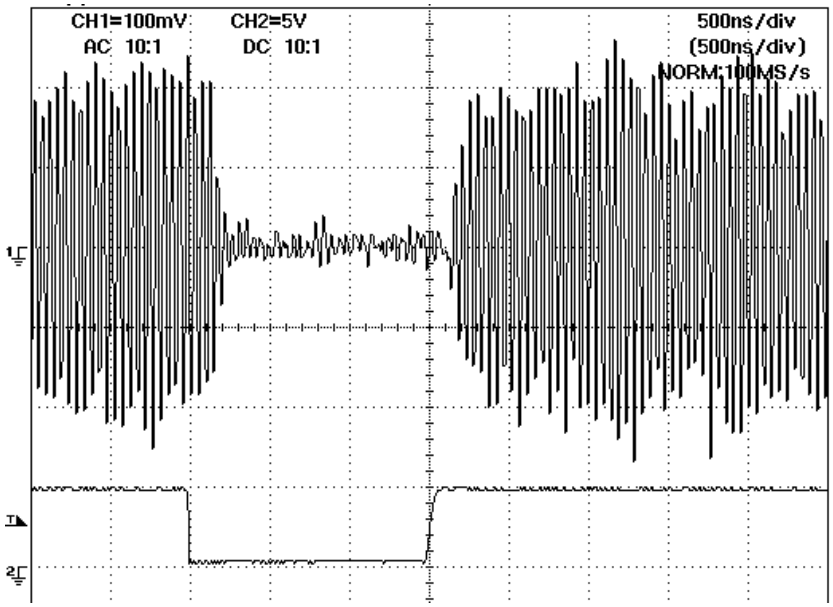

Figure 3-26. Detailed OOK transition

The bottom line is the modulation data. The implementation of the OOK transmitter was done using the same driver than the BPSK transmitter. Changing only the digital signal that controls the driver gate. In the phase shift case we had 180 degrees change of phase. In the OOK case the gate is open during the OFF time and during the ON time, the gate switches at the frequency that matches the coil impedance.

The strong dependence of OOK modulation with coil-to-coil distance and orientation makes this communication technique very difficult, and by far less reliable than the BPSK. Although in some cases with strong S/N in the receiver this alternative may be useful.

In addition to the OOK modulation and in order to provide an extremely low-power on-chip transmitter a novel technique was investigated, and it is presented in next section.

3.2.2.3.2 "LC-modulation" technique

In the above BPSK transmitter the current consumption is defined by the amount of charge that the NMOS source delivers to the coil. In order to have higher magnetic field we have seen than the stimulation current should match the coil impedance, so during every carrier cycle some current is spent. A new proposal is what we call LC technique, were the excitation energy does not try to match the resonance of the coil, but just induce a sharp oscillation peak at a given time, producing a wide band burst with peak frequency centered in the self-resonance of the LC tank.

Dumping a certain amount of energy in a highly tuned resonant LC circuit produces a sharp oscillation response, with an amplitude decay dependent on the Q. The higher the Q the higher the amplitude peak and the longer the time the oscillation to dissipate. If the received Signal-to-Noise ratio of the peak is acceptable then the communication becomes possible. Modulating the information with PPM (Pulse Position Modulation) data can be sent from the implant to the external unit with extremely low power consumption. Every transition in the data line causes an abrupt oscillation signal with a frequency defined by the LC value of the coil plus capacitances seen by the coil (see figure 3-27). So the self-resonance frequency can be adjusted simply changing the capacitance value without requiring any circuit effort, because there is no carrier signal generated. The envelope decay is defined by the capability of the LC tank to dissipate the energy, thus the larger the coil resistance the faster the decay.

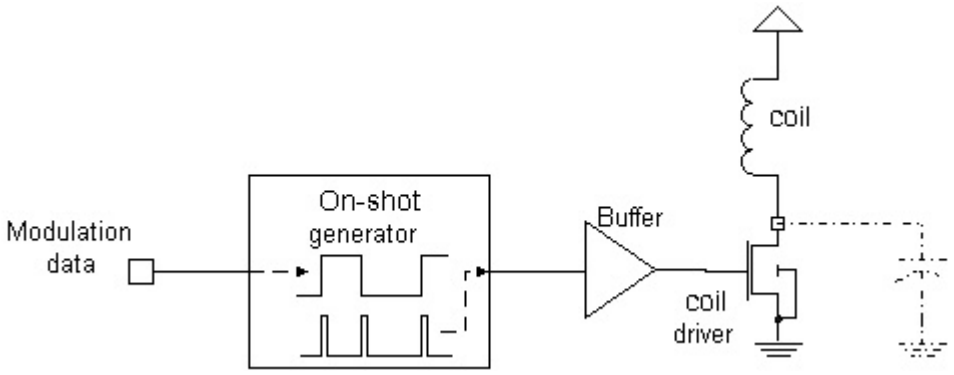

Figure 3-27. LC transmitter

Figure 3-28 shows the on-chip transmitter signal and figure 3-29 shows the received signal at 10mm of distance. In the transmitter we see that every time the data line changes (upper signal) there is a clean 500ns/decay signal of about 20MHz of self-oscillation. Right picture shows the received signal with a signal-to-noise ratio of about 6 (natural units) or 15.6dB for a distance of 10mm.

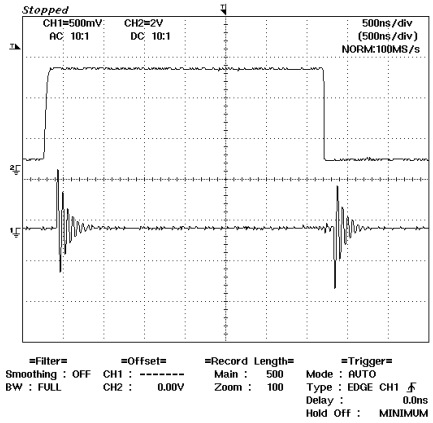

Figure 3-28. <1uW transmitted LC signal

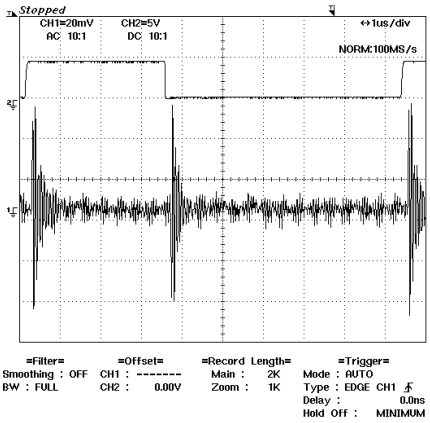

Figure 3-29. Received signal at 10mm

The power required to transmit the data using this technique is extremely small (measured bellow 1uW). The first reason is because we do not require any high frequency oscillator providing the carrier signal, and secondly because we only inject charge in the tank once per transition.

3.3 REFERENCES

[1] FCC rules and regulations , part 15

[2] Mischa Schwartz, "Information transmission, modulation and noise", McGraw-Hill, 1980, pp. 212-231.

[3] D.R. Smith, "Digital Transmission Systems, 2nd Ed.", Van Nostrand Reinhold, 1993.

[4] C.E. Shannon, "Communication in the Presence of Noise.", *Proc. IRE*, vol. 37, pp. 10-21, January 1949.

[5] J. Ji, K.D. Wise, "An implantable CMOS circuit interface for multiplexed microelectrode recording arrays." *IEEE Trans. Biomed. Eng.*, vol. 27, no. 3, pp. 433-443, March 1992.

[6] C.D. Slocum, V.T. Cutolo, "Analog telemetry system for biomedical implant", U.S. Patent No. 4,543,953, Oct. 1, 1985.

[7] E.P. McCutcheon, et. al, "An inductively powered implantable multichannel telemetry system for cardiovascular data.", Biotelemetry III, *Proc. Int'l Symp. on Biotelemetry*, pp. 71-74, Academic Press, 1976.

[8] F.B. Shapiro, "An integrated circuit for biotelemetry with digital IC sensors", Ph.D. Dissertation, Stanford University, 1989.

[9] Harold S. Black, "Modulation Theory", D. Van Nostrand Co., 1953, pp. 263-298

[10] T.B. Fryer, R.M. Westbrook, "A multichannel biotelemetry transmitter utilizing a PCM subcarrier.", Biotelemetry II, *Proc. Int'l Symp. on Biotelemetry*, pp. 202-204 , S. Karger, 1974.

[11] A.M. Leung, et al., “Intracranial pressure telemetry system using semicustom integrated circuits.”, *IEEE Trans. Biomed. Eng.*, vol. 33, no. 4, pp. 386-395, April 1986.

[12] J.J. Cupal, R.W. Weeks, “Digital encoding techniques for the telemetering of biological data.” Biotelemetry X, *Proc. Int’l Symp. on Biotelemetry*, pp. 39-50, University of Arkansas Press, 1989.

[13] M.K. Kazimierczuk, "Collector Amplitude Modulation of the Class-E Tuned Power Amplifier", IEEE Transactions on Circuits and Systems, Vol. CAS-31, Nº 6, pp. 543 - 549, June 1984.

[14] M. Nardin, K. Najafi, “A multichannel neuromuscular microstimulator with bi-directional telemetry”, 8th conference on solid-state sensors and actuators, 59-62, June 95

[15] C. Zierhofer, E. Hochmair, “High-efficient coupling-insensitive transcutaneous power and data transmission via an inductive link”, IEEE transactions on biomedical engineering, vol.37, nº7, 716-722 July 95

[16] J. Parramon, N. Barniol, J. Oliver, E. Valderrama, "RF powered implantable telemetry system", XIV Congreso de la sociedad española de ingeniería biomédica, Navarra (Spain), Sep.96

[17] D. Marín, I. Martínez, E. Valderrama, J. Aguiló."Very high data bit rate for implantable and RF-powered stimulators through a transcutaneous telemetry link". International Society on Biotelemetry, ISOB99, Alaska, May 1999.

[18] E.Vittoz, J. Fellrath, “CMOS Analog Integrated Circuits based on weak inversion operation”, IEEE Journal of solid-state circuits, VOL.SC-12, No.3, June 1977

[19] R.Puers, K. Van Shuylenbergh et al., “IMPACT: Implant Monitoring Project using ACtive Telemetry”, BRITE-EURAM CT90-0323, 1995

[20] B. Ziaie, M. Nardin, J. von Arx, K Najafi, “A single channel implantable microstimulator for functional neuromuscular stimulation”, 7th conference on solid-state sensors and actuators, 450-453, June 93

[21] K. Van Shuylenbergh, R. Puers, “Passive telemetry by harmonics detection”, 18th Conference of the IEEE EMBS, 1.7.2 telemetry II session, Nov’96

[22] Z. Tang, B. Smith, J. Schild, P. Hunter, “Data transmission from an implantable biotelemeter by load-shift keying using circuit configuration modulator”, IEEE transactions on biomedical engineering, vol.42, nº5, May95

[23] Tayfun Akin, “An integrated telemetric multichannel sieve electrode for nerve regeneration applications”, Thesis dissertation, The university of Michigan, Ann Arbor, pp 69

[24] Allen&Holdberg, DAC section